Development 122, 2955-2963 (1996)
Printed in Great Britain © The Company of Biologists Limited 1996
DEV8340

Mutations in the 8 kDa dynein light chain gene disrupt sensory axon projections in the *Drosophila* imaginal CNS

R. Phillis, D. Statton, P. Caruccio and R. K. Murphey*

Department of Biology and Graduate Program in Molecular and Cellular Biology, Morrill Science Center, University of Massachusetts, Amherst, MA 01003, USA

*Author for correspondence (e-mail rmurphey@bio.umass.edu)

SUMMARY

Mutations in an 8 kDa (8×10^3 M_r) cytoplasmic dynein light chain disrupt sensory axon trajectories in the imaginal nervous system of *Drosophila*. Weak alleles are behaviorally mutant, female-sterile and exhibit bristle thinning and bristle loss. Null alleles are lethal in late pupal stages and alter neuronal anatomy within the imaginal CNS. We utilized P[Gal4] inserts to examine the axon projections of stretch receptor neurons and an *engrailed-lacZ* construct to characterize the anatomy of tactile neurons. In mutant animals both types of sensory neurons exhibited altered axon trajectories within the CNS, suggesting a defect in axon pathfinding. However, the alterations in axon trajectory did not prevent these axons from reaching their normal termination regions. In the alleles producing these neuronal phenotypes, expression of the cytoplasmic dynein 8 kDa light chain gene is completely absent. These results demonstrate a new function for the cytoplasmic dynein light chain in the regulation of axonogenesis and may provide a point of entry for studies of the role of cellular motors in growth cone guidance.

Key words: dynein, enhancer trap, P[Gal4], *engrailed-lacZ*, *Drosophila*, sensory axon, CNS

INTRODUCTION

The molecular mechanisms underlying the assembly of selective synaptic connections are currently under intense scrutiny. Recent genetic approaches in the worm (Hedgecock et al., 1990; McIntire et al., 1992) and the fly (Seeger et al., 1993; Van Vactor et al., 1993; Martin et al., 1995; Kania et al., 1995) have identified some of the genes that direct specific patterns of axon growth. Characterization of these genes and their products is revealing a variety of molecules involved in axon guidance and the assembly of the nervous system. These range from molecules that attract or repel growth cones from a distance, such as the netrins (Kennedy et al., 1994; Colamarino and Tessier-Lavigne, 1995; Matthes et al., 1995), through a group of cell surface molecules involved in growth cone steering such as fasciclin II (Grenningloh et al., 1991; Lin and Goodman, 1994; Chiba et al., 1995), to molecules that interact with the cytoskeleton and may function in the dynamics of growth cone shape changes required for directional growth of axons (Tanaka and Sabry, 1995).

Much of the work in *Drosophila* is focused on the embryo, where a wide array of immunological, genetic and molecular probes have been developed for visualizing specific aspects of neuronal anatomy (Seeger et al., 1993; Van Vactor et al., 1993; Martin et al., 1995; Salzberg et al., 1994; Kania et al., 1995). These methods have allowed detailed examination of axon pathfinding, both within the embryonic CNS (Seeger et al., 1993; Nose et al., 1992) and in the periphery (Kania et al., 1995; Van Vactor et al., 1993). Analysis of the imaginal CNS is much less well developed because similar anatomical probes are not available. Historically, mutations in adult function were isolated in screens for behavioral defects and then characterized for corresponding anatomical defects using various classical neuroanatomical methods (e.g. Thomas and Wyman, 1982). In other screens neuroanatomical defects were the primary focus and mutants were subsequently tested for behavioral changes (Fischbach and Heisenburg, 1984). The P[Gal4] enhancer traps (Brand and Perrimon, 1993; Smith and Shepherd, 1996), and a variety of promoter-fusion constructs like *engrailed-lacZ* (Hama et al., 1990), are now providing the crucial tools for studying anatomical defects in mutant imaginal nervous systems.

Within the neuropil of the imaginal CNS there are distinct synaptic fields that have been resolved using classic dye injection methods (Pfluger et al., 1988; Murphey et al., 1989b; Merritt and Murphey, 1992). Different types of sensory neurons arborize in specific domains of the CNS that subserve different modalities of sensory input. These domains are related to synaptic connectivity with the target neurons (Killian et al., 1993). This organization provides a unique phenotype in which to screen for mutations in synaptic connectivity. By combining P[Gal4] enhancer traps with behavioral screens in adults, we have found a new mutation that affects the assembly of the imaginal nervous system.

We have used two P[Gal4] insertions (Brand and Perrimon, 1993) and an *engrailed-lacZ* reporter construct to characterize

the effects of mutations in a gene called *cut up* (*ctp*) on the central projections of imaginal sensory neurons. We show that mutations in this gene alter axon projections, causing them to follow abnormal pathways within the CNS. However, *ctp* mutations do not prevent the sensory neurons from terminating within their normal target domain. Molecular characterization of this gene reveals that it encodes the 8 kDa dynein light chain. This result revealed a role for this small subunit of cytoplasmic dynein in establishing axon trajectories and provides a new point of entry for studies of the dynein complex in axon pathfinding.

MATERIALS AND METHODS

Genetics

The original allele, *ctp*^{1}, was isolated as a P[lacW] insertion (Bier et al., 1989) on the *w*^{bio} X chromosome (Phillis et al., 1993). Excision alleles were generated using Δ2-3 according to standard methods (Robertson et al., 1988). All *ctp* stocks were maintained over the balancer FM7c. Deficiency stock Df(1)RL40 used in complementation tests was obtained from the Bloomington Drosophila Stock Center. The *engrailed-lacZ* contruct was maintained over CyO and obtained from Tom Kornberg. The P[Gal4] insertions, c62 and c362, were recombined onto chromosomes carrying a P[UAS-*lacZ*] to create chromosomes that could be easily crossed into *ctp* mutant genetic backgrounds in a single generation. All flies were maintained at room temperature on standard cornmeal molasses medium.

Molecular biology

The genomic library used to isolate the original *ctp* clone was prepared using the genomic DNA from *ctp*^{1} and the vector lambda-GEM11 (Promega). The library was screened with pπ25.7wc sequences as a probe using standard techniques (Sambrook et al., 1989). *Sac*I fragments from the genomic clones were subcloned into pBKS+. A late stage embryo cDNA library in λgt11 was obtained from Kai Zinn, and probed with the subclones using standard techniques. Sequence analysis was performed by Retrogen Inc. Northern blots were loaded with 5 μg poly(A)$^+$ RNA and probed with cDNA sequences labeled by random priming.

Immunocytochemistry

The thoraco-abdominal nervous system was removed from heterozygous pupae, (*ctp* males carrying one copy of the P[Gal4] UAS recombinant chromosome) approximately 70 hours after pupariation at 22°C. The CNS was dissected into 0.1 M phosphate buffer, fixed in 4% paraformaldehyde overnight at 4°C, washed in 0.1 M phosphate buffer, incubated in 2 N HCl in phosphate buffer and Triton-X (0.4%) (PBTX) for 30 minutes, then washed in several changes of PBTX. The tissue was then blocked in 3% normal horse serum in PBTX for 1 hour and incubated overnight in primary antibody (anti-β-galactosidase; Promega) at 1:500 with 3% horse serum and phosphate buffer. Specimens were washed in 0.1 M PBTX and stained according to the ABC kit from Vector Labs.

Images in Figs 1, 2 and 3 represent composites of in-focus regions of micrographs taken at a series of focal planes through the preparations. Images in Figs 1C,D, and 2C,D, represent composites prepared from images of successive sections through the preparations. Regions of the image were selected that contained the relevant stained axons. Manipulations were performed in Photoshop® on images scanned from 35 mm slides.

RESULTS

Isolation of the *cut up* mutation

The original *cut up* allele, *ctp*^{1}, was identified among a group of X-linked P[lacW] insertion lines that were screened for defects in grooming behavior according to the methods of Phillis et al. (1993). The *ctp*^{1} allele caused mild defects in grooming but produced no obvious defects in other coordinated behaviors such as walking or flying. The insertion also caused subtle changes in the external structure of sensory receptors; producing thinner and shorter macrochaetae on notum and legs, occasional loss of notal macrochaetae and reduction in the number of notal microchaetae to approximately 75% of wild type. Finally, the *ctp*^{1} mutation was female-sterile.

The P[lacW] insertion site in *ctp*^{1} was mapped, by *in situ* hybridization, to polytene chromosome band 4D1-3 and deficiencies deleting this region failed to complement the bristle phenotypes (Table 1). The deficiency complementation tests also suggested that *ctp*^{1} was a weak hypomorphic allele, since the bristle phenotype of the *ctp*^{1}/Df(1)RL40 hemizygous females was more severe than was observed for *ctp*^{1} homozygotes. Additional alleles of *ctp* were generated through imprecise excision of the P element insertion. Of the 79 independent excisions recovered, we obtained six lethals, 53 viable alleles with mutant bristle phenotypes and 20 wild-type revertants. We selected some of these alleles (see Table 1) for detailed analysis of *ctp* effects on neuronal anatomy.

We recovered six independent excision alleles in which there were no male or homozygous female adult survivors. All of these alleles failed to complement *ctp*^{1} with respect to the bristle phenotype. For further study we selected two of these alleles, *ctp*^{e55} and *ctp*^{e73}, which behaved genetically as null mutants, where heterozygous *ctp*^{1}/*ctp*^{e73} or *ctp*^{1}/*ctp*^{e55} females had bristle defects indistinguishable from *ctp*^{1}/Df(1)RL40. Neither of these alleles showed dominant phenotypes over wild type in heterozygous females. The *ctp*^{e73} and *ctp*^{e55} mutants failed to eclose as adults, but most survived to late pupal stages, where they exhibited CNS defects (see below) and had bristle defects characteristic of the strongest viable *ctp* alleles. We also recovered 20 revertant alleles that were wild type with respect to all characters for which we have observed defects in mutant *ctp* alleles, including bristle morphology and interallelic complementation (Table 1). Two of these revertant excision alleles, *ctp*^{e21} and *ctp*^{e27}, have been used as controls in our characterizations.

Table 1. Phenotypes of cut up alleles used in this analysis

	Defective characters		
Allele	Bristle thinning[1]	Microchaete density[2]	Viability[3]
ctp^1/*ctp*^{1}	–	–	+
ctp^1/Df(1)RL40	– –	– –	+/–
ctp^{e73}/*ctp*^{e73}	– –	– –	–
ctp^1/*ctp*^{e73}	– –	– –	+/–
ctp^{e55}/*ctp*^{e55}	– –	– –	–
ctp^{e21}/*ctp*^{e21}	+	+	+
ctp^{e27}/*ctp*^{e27}	+	+	+

[1]Bristle thinning was scored as (+) for wild type, (–) for mild thinning of macrochaetae on head and notum, and (– –) for moderate thinning of macrochaetae on head, notum and legs.

[2]Microchaete density was scored as (+) for wild type, (–) for mild thinning of notal microchaetae, ~75% of wild-type number, and (– –) for moderate thinning of notal microchaetae, ~50% of wild-type number.

[3]Viability was scored as (+) for wild type, (+/–) for fewer than 50% of expected adults, and (–) for no eclosing adults.

ctp affects the axon projections of imaginal sensory neurons

Tactile neurons

Since *ctp*^{1} was isolated using an assay of tactile function (Phillis et al., 1993), we examined the axonal projections of tactile sensory neurons in *ctp* null mutants. The anatomy of the sensory neurons associated with the mechanosensory bristles of adults was revealed by the *engrailed-lacZ* fusion construct *ryXho25*, which is expressed in the cells of the posterior compartment of each segment (Hama et al., 1990). We have found that antibodies to the β-galactosidase expressed by *en-lacZ* label the axonal projections of the posterior tactile neurons, allowing them to be visualized with standard immunohistochemical techniques (Fig. 1A). No projections from other sensory neurons such as campaniform or chordotonal neurons (see below) were stained by this construct.

The bundle of axons from the *en-lacZ*-expressing neurons projects through each main leg nerve into the pupal thoracic CNS (Fig. 1A, large arrowhead). Upon entry into the CNS, these tactile axons project primarily along the posterior trajectory described for tactile axons in the posterior compartment (Fig. 1A, arrows; see also Murphey et al., 1989a). In addition, a small minority of the *en-lacZ* labeled axons exhibit an anterior trajectory (Fig. 1A). These anteriorly projecting axons correspond to the tactile neurons that lie just anterior to the compartment boundary in the leg (Murphey et al., 1989a). In transverse section, the *en-lacZ*-labeled axons are seen to lie immediately adjacent to the ventral surface of the neuropil in each neuromere (Fig. 1D), consistent with their tactile function (Murphey et al., 1989b). Within the CNS, expression of the *en-lacZ* element is also observed in a group of cell bodies near the ventral midline in each neuromere (Fig. 1A,B). Expression of *engrailed* in these cells has been previously observed in preparations from both *Drosophila* and locust (Siegler et al., 1993). The axons and dendrites from these somata stain very weakly in our preparations and do not interfere with visualization of the axon projections of tactile sensory neurons.

In *ctp*^{e73} late pupal nervous systems, the axons from many of the *en-lacZ*-positive sensory neurons projected abnormally within the pupal CNS, extending along an anterior pathway (Fig. 1B, double arrowheads). When the anterior bundle was large, the number of axons in the posterior region appeared to be reduced (Fig. 1B, single arrow), consistent with a change in the axons from a posterior to an anterior trajectory. In a few cases, the normal posterior projections from *en-lacZ*-positive neurons were completely absent, and only the anterior projections were observed (not shown). This axon trajectory phenotype was highly penetrant in *ctp*^{e73} mutants; 37 of 38 specimens exhibited abnormal projections in at least one of the thoracic hemi-neuromeres. An average of 4.0 hemi-neuromeres per CNS showed the mutant phenotype. These axon phenotypes were never observed in preparations from the revertant allele *ctp*^{e21} (0 of 29 specimens). In addition, we examined these axons in a Canton-S background and never saw abnormal projections.

Errors in tactile axon targeting were further characterized in sections of the CNS of some of the *en-lacZ*-stained *ctp*^{e73} mutant preparations. Previous analyses of wild type have shown that the tactile axons terminate in a ventral layer of the leg neuropil (Murphey et al., 1989a,b). In the mutant specimen illustrated, sections through the normal posterior tract show that the axons arborize in the ventral layer of the neuropil just as in the wild-type tactile sensory neurons (Fig. 1D, arrows; see also Murphey et al., 1989a). In the anterior region of this mutant prothoracic neuromere, where the aberrant projections

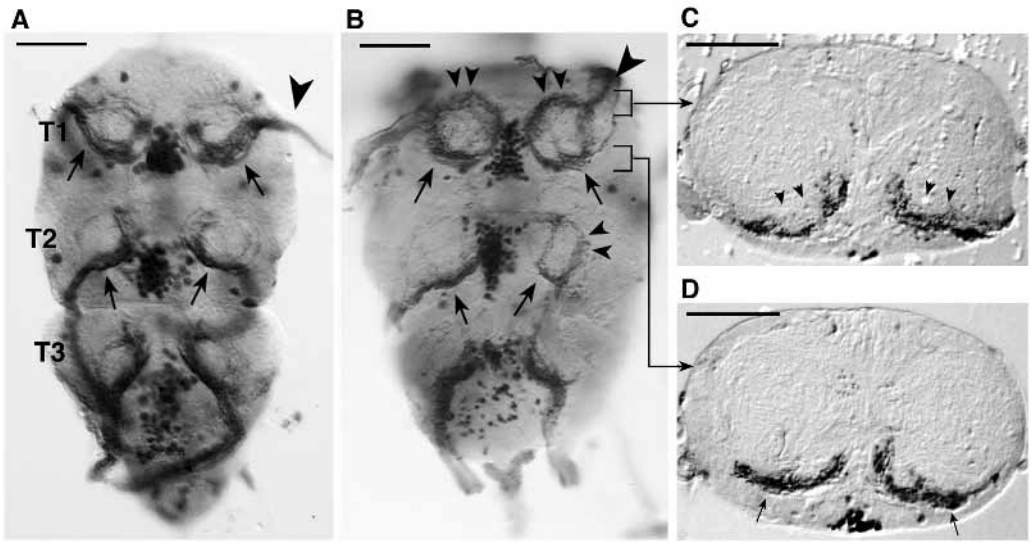

Fig. 1. *ctp* mutations alter the axon trajectories of tactile neurons. (A) Wild-type (*ctp*^{e21}) axonal projections in a whole-mount of the thoracic nervous system. Antibodies to β-galactosidase in specimens carrying the *engrailed-lac Z* construct, ryXho25 (Hama et al., 1990) label primarily the posterior leg tactile axons, which enter the CNS through the main leg nerve (large arrowhead). The main posterior bundle of axons is labeled (single arrow) as well as a few axons that run on an anterior tract. A group of central somata on the ventral surface of each neuromere is also labeled. The pro- (T1), meso- (T2) and metathoracic (T3) neuromeres are indicated and anterior is at the top. (B) The axonal projections in a pupal lethal, *ctp*^{e73}, nervous system. Note the enlarged anterior bundle of axons in the pro- and mesothoracic neuromeres (double arrowheads). The anterior projections in *ctp*^{e73} lead to a reduction in the density of the axons, making the posterior projections smaller than normal (single arrows). C and D) Transverse sections of the prothoracic neuromere of the specimen shown in B. C) Reconstruction of the anterior tract of axons (a composite of three 7 μm transverse sections for the region indicated by the bracket). The axons arborize only in a ventral layer of neuropil known as the lateral Ventral Association Center (arrowheads). (D) Reconstruction of the posterior tract of axons (a composite of three 7 μm transverse sections for the region indicated by the bracket). Note that these axons arborize ventrally just as they do in wild-type specimens (arrows) (Murphey et al., 1989a).

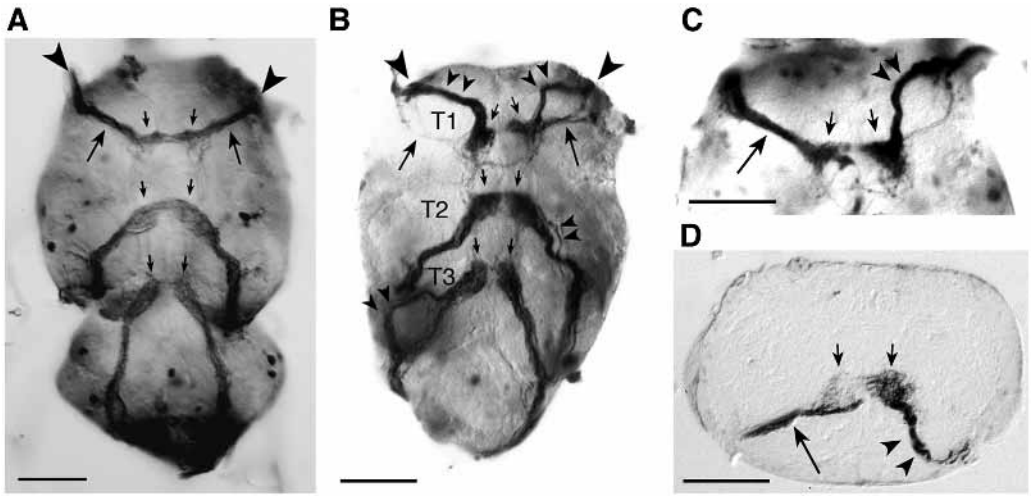

Fig. 2. *cut up* mutations alter the axon trajectories of the club-like femoral chordotonal organ axons. (A) Wild-type nervous system (*ctp*^{e21}). Antibodies to β-galatosidase in mutants carrying a P[Gal4] insertion labeled axons that enter the CNS through the main leg nerve (arrowhead). These axons run on the oblique tract (large arrows) and terminate in a region known as the mVAC (small arrows). (B) The pupal lethal *ctp*^{e73} nervous system. Note the axon trajectory is now shifted anteriorly in the prothoracic neuromere (double arrowheads) but the axons terminate in the normal target region (small arrow). A few axons remain on the normal tract in this neuromere (large arrows). In the second and third thoracic neuromere, axons can be seen to defasciculate from the main bundle (double arrowheads). (C) Whole-mount of the *ctp* nervous system in another specimen, showing the prothoracic neuromere. Note the strong anterior deflection of most axons in the right neuromere (double arrowheads), the normal trajectory in the left neuromere (large arrow) and the endings of axons in similar positions in each neuromere (small arrows). (D) Reconstruction of transverse sections of the axonal termination region of the specimen shown in C (a composite of eight 7 μm sections through the prothoracic neuromere; dorsal is at the top). The axons in the left hemi-neuromere are on the normal oblique tract (large arrow); the axons in the right hemi-neuromere follow an unusual ventral trajectory (double arrowheads), but terminate in the mVAC (small arrows).

are observed, the axons also lie in the ventral layer of the neuropil (Fig. 1C, double arrowheads). Thus *ctp* alters tactile axon trajectories but does not alter the domain of axon termination.

Chordotonal neurons

To assess *ctp* function further, we examined its affect on the axons of three distinct classes of stretch receptors, two from the femoral chordotonal organ (feCO) and one from the anterior chordotonal organ (aCO). P[Gal4] insertions that were expressed in these subsets of sensory neurons were used to drive a UAS-*lacZ* reporter gene and the expression was revealed with antibodies to β-galactosidase (Smith and Shepherd, 1996; S. Reddy and R. K. Murphey, unpublished data). A detailed analysis of the axon projections and behavioral function of these chordotonal organs will be reported elsewhere (S. Reddy and R. K. Murphey, unpublished data).

The club neurons of the femoral chordotonal organ

One subset of the feCO neurons extends projections into the CNS in the shape of a club. These neurons can be visualized using the P[Gal4] enhancer trap insertion c62, which is expressed in these sensory neurons in late-stage pupae. In wild-type specimens, the club neurons extend axons into the CNS through the main leg nerve (Fig. 2A, arrowheads), cross the neuromere on the oblique tract (Fig. 2A, large arrows), and terminate in a club-like structure (Fig. 2A, small arrows) called the medial Ventral Association Center (mVAC) (Pfluger et al., 1988; Field and Pfluger, 1989). In addition, some of the axons extend intersegmentally to the mVAC in adjacent neuromeres.

In *ctp*^{e73} mutants, the club neurons often exhibited a deflection of the main axon bundle from the oblique tract toward the anterior edge of the neuropil (Fig. 2B, double arrowheads). A subset of the axons projected in the normal manner along the oblique tract (Fig. 2B, large arrow), while others projected abnormally along an anterior trajectory (Fig. 2B, double arrowheads). This defect was observed in one or more hemi-neuromeres in 15 of 23 preparations. The majority of the preparations (13 of the 15 with abnormalities) showed the defect exclusively in the prothoracic hemi-neuromere. We also observed occasional splitting of the axon bundles as they crossed the neuromere on the oblique tract (Fig. 2B, double arrowhead in the second thoracic neuromere). However, in all cases the deflected axons still showed the expansion and termination of the axon bundle in mVAC (Fig. 2B, small arrow). These axon trajectory errors were never observed in the revertant excision line, *ctp*^{e21} (0 out of 46 preparations), nor did we find abnormal projections in a Canton-S background.

Transverse sections confirmed that the deflected feCO axons follow an unusual ventral trajectory but still terminate in the mVAC. In the specimen illustrated, these axons follow the ventral surface of the ganglion and then curve dorsally (Fig. 2D, double arrowheads) to terminate in the mVAC (Fig. 2D, small arrows). In this example, the axons in the left prothoracic hemi-neuromere follow the normal trajectory, passing along the oblique tract and terminating in the mVAC (Fig. 2C,D, large arrows).

Anterior chordotonal neurons

A second P[Gal4] insert, c362, is expressed in two types of stretch receptors: the anterior chordotonal organ of Power (1948) and a group of neurons from the feCO. The anterior chordotonal organ (aCO) is a small thoracic structure containing approximately 20 cell bodies located in the ventral body cavity adjacent to the CNS (Fig. 3, arrow labeled aCO). Axons from the aCO enter the prothoracic ganglion via the aCO nerve, project obliquely across the prothoracic neuromere (Fig. 3A,B, arrows labeled aCO), enter one of the longitudinal interseg-

mental tracts and terminate in the dorsal mesothoracic neuromere (Fig. 3, asterisk).

In *ctp*^{e73} mutants, the aCO axons were often deflected to an anterior tract as they crossed the T1 neuromere (Fig. 3B). When analyzed by hemi-neuromere, 47 specimens gave the following data: 69 of the hemi-neuromeres exhibit axon bundles in the incorrect, anterior position, and 23 were in the wild-type location (two hemi-neuromeres could not be scored). In spite of the altered trajectory, the aCO axons did reach an intersegmental tract and project posteriorly to terminate in the dorsal mesothoracic region (Fig. 3B, asterisk). Such deflections were never observed in *ctp*^{e21} control preparations (0 out of 31 preparations).

The claw-like neurons of the femoral chordotonal organ

The c362 insert also labels a subset of feCO neurons that are distinct from the club neurons described above. These neurons project into each thoracic hemi-neuromere via the main leg nerve and send branches in a distinctive claw-like pattern into each of three regions: the anterior and posterior lateral association centers and a region anterior and dorsal of the mVAC (Fig. 3A). In transverse section, all three termination regions are in a layer of neuropil thought to be the processing area for proprioceptors (S. Reddy and R. K. Murphey, unpublished data; Murphey et al., 1989b).

The axon projection pattern of the claw neurons was also altered in *ctp*^{e73} mutants. The characteristic claw-like pattern was often distorted by the alteration, addition or deletion of branches (Fig. 3). Axon bundles were defasciculated, splaying across broad regions of the neuropil (Fig. 3). The effects of *ctp*^{e73} were highly penetrant; 49 of the 50 preparations showed some type of axonal abnormality associated with the claw feCO axons. In addition, defects were observed in an average of 5.1 hemi-neuromeres per specimen. In contrast, only one of 24 of the *ctp*^{e21} controls showed any abnormality in the projection pattern of the claw-like feCO axons.

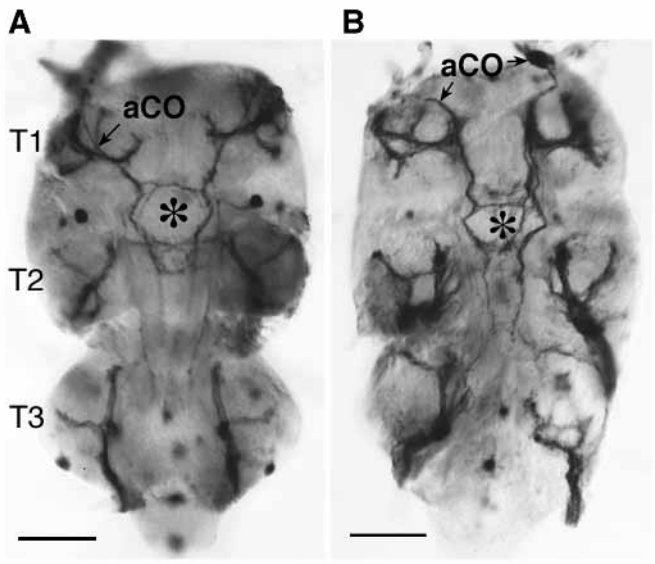

Fig. 3. *cut up* mutations alter the axon trajectories of two groups of stretch receptor axons: the claw axons from the feCO and the axons of the anterior chordotonal organ. (A) Wild-type nervous system (*ctp*^{e21}). The anterior chordotonal organ axons enter through a small anterior nerve, cross the neuropil of the prothoracic neuromere (single arrow labeled aCO) and terminate in the mesothoracic flight neuropil (asterisk). The claw axons enter the CNS through the main leg nerve in each segment, branch and terminate in three areas of each leg neuropil. (B) *ctp*^{e73} mutant specimen. Within the prothoracic neuromere, the aCO axons are deflected onto an anterior tract (small arrows labeled aCO). However the termination region (asterisk) appears relatively normal. In addition, the claw pattern of projections is distorted in the mutants, for example compare the left T2 neuromere in the two specimens.

To verify that the *ctp* axon phenotypes we observed were not unique to the *ctp*^{e73} and *ctp*^{e21} alleles, we analyzed the CNS from pupae carrying the lethal allele *ctp*^{e55}, or the wild-type revertant allele *ctp*^{e27}. The same types of projection errors documented above for *ctp*^{e73}, were observed in the *ctp*^{e55} mutants and at similar frequency. The tactile axons visualized using *en-lacZ* showed abnormal anterior arborizations in 10 of the 12 preparations. The club neurons of the feCO followed unusual tracts in 10 of 11 preparations. The aCO axons followed an abnormal anterior tract like those observed for *ctp*^{e73} in 15 out of 15 CNS preparations sampled. The feCO claw axons showed branching errors and defasciculation in 15 out of 15 preparations. Thus *ctp*^{e55}, an independent lethal excision allele, showed the same axon phenotypes as *ctp*^{e73}. Similarly, though with smaller samples, revertant allele *ctp*^{e27} was consistently wild type, reinforcing the results obtained with revertant allele *ctp*^{e21}.

The gross anatomy of the *ctp* mutant nervous systems was clearly distorted. In pupae of *ctp*^{e73}, the T3 neuromere was compressed anteriorly and the constriction between the T3 and T2 neuromeres lost (see Figs 1, 2 and 3). In addition, the *ctp*^{e73} imaginal CNS appears smaller than wild type. However, several central cell bodies that express the *en-lacZ* marker do not appear to be altered in position (see Fig. 1). Further, the structure of the CNS is intact enough that sensory neurons enter through appropriate nerves and arborize in correct segments.

Embryonic CNS

Anti-HRP staining of *ctp*^{e73} embryos revealed defects in the organization of the CNS in a small fraction of specimens. In 25 out of 318 mutant embryos the central axon fascicles were severely disrupted. These disruptions included defects in the longitudinal connectives and commissural tracts. In these animals there is also evidence of disruptions in the peripheral nervous system, seen most clearly as loss or misrouting of the segmental and intersegmental nerves. In the remaining *ctp* ^{e73} embryos, no defects in CNS morphology were detectable. The low frequency of defects visible at this level of resolution suggest either that the embryonic defects are subtle and difficult to resolve with anti-HRP staining, or that most defects are manifested later in development, and become visible in assays of the imaginal CNS.

Cloning *ctp*

We made use of two features of the original *ctp* allele to assist our recovery of the *ctp* clone. The original allele is a P element insertion allele, and allowed recovery of genomic sequences adjacent to the insertion site by transposon tagging. The *lacZ* reporter in the P[lacW] element showed a strong expression pattern restricted to the CNS and some cells of the PNS after embryonic stage 15. In larval and pupal stages, expression was

nearly uniform in the imaginal discs and the CNS. In our screen for cDNAs, we isolated clones that had both homology to genomic clones from the P element insertion site and identified transcripts with patterns of expression similar to the enhancer trap pattern. We then assayed the expression of the transcripts identified by the cDNA clones in mutants to verify that our genetic null alleles had disrupted expression.

We prepared a genomic library using DNA from the *ctp*^{1} stock and screened it with P element sequences. We recovered four overlapping genomic clones containing sequences adjacent to the P element insertion site that were 14 to 18 kb in length. Subclones from these genomic clones were used to screen a cDNA library prepared from mid- to late-stage embryos (obtained from Kai Zinn) and two cDNA clones were recovered. One of the clones was a 1.5 kb cDNA that identified two transcripts on northern blots, of 1.8 kb and 4.3 kb. This cDNA was used in wholemount *in situ* hybridization to embryos. The 1.5 kb cDNA clone hybridized to all cells of the CNS and to the group of lateral scolopidial organs of the PNS of late-stage embryos (Fig. 4B). This pattern of expression is very similar to the enhancer trap expression pattern observed for the P[lacW] element inserted into *ctp*^{1} (Fig. 4A). Northern blots of RNA prepared from *ctp*^{e73} embryos show that both the 1.8 kb and 4.3 kb transcripts are completely deleted in these mutants (Fig. 5). These two transcripts are unaffected in the revertant allele *ctp*^{e21}. The P element insertion in *ctp*^{1} is within 1 kb of the transcribed region, and the excision allele *ctp*^{e73} deletes approximately 1 kb of genomic sequences that include sequences from the 5′ end of the transcribed region (Fig. 6A).

cut up encodes the dynein light chain

Sequence analysis of the 1.5 kb cDNA clone shows a predicted open reading frame of 89 amino acids. Conceptual translation of this sequence shows it has over 95% amino acid identity with the 8 kD dynein light chain from Chlamydomonas (Fig. 6B) (King and Patel-King, 1995). A sequence from the *C. elegans* data base shows very strong homology as well. Several STS entries into the sequence databases from humans and mouse also show very strong homology to the *ctp* sequence. This subunit of dynein is found in both flagellar and cytoplasmic dynein in Chlamydomonas (King and Patel-King, 1995).

The *Drosophila* dynein light chain gene was recently identified independently by Dick et al. (1996). These authors called the gene *Ddlc1* and show that partial loss of function alleles are female-sterile. In order to verify that *Ddlc1* and *ctp* are the same gene, we performed complementation tests. *Ddlc1* mutations

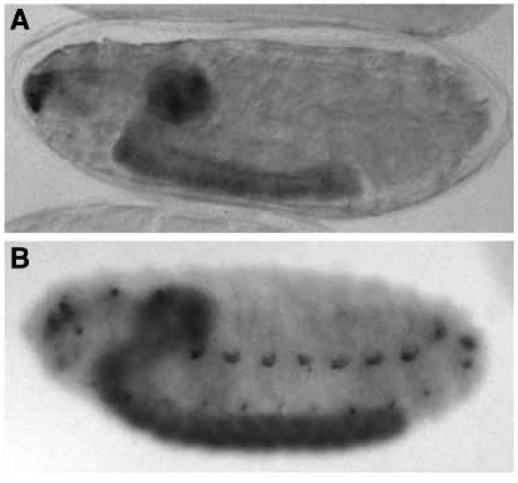

Fig. 4. *ctp* is expressed in the embryonic CNS and a subset of the embryonic sensory neurons. (A) Enhancer trap expression pattern from the P[lacW] insertion in *ctp*^{1}. Staining is observed throughout the CNS and in the antennomaxillary sensory organs. (B) Expression of the *ctp* gene in embryos. Stage-15 embryo after *in situ* hybridization of *ctp* 1.5 kb cDNA clone showing expression within the CNS, the antennomaxillary complex, and the lateral chordotonal organs.

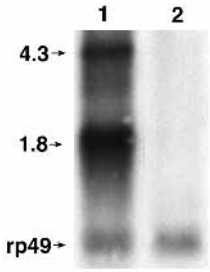

Fig. 5. Northern blot comparing *ctp* expression in mutant and wild type. Each lane contains 5 μg of poly(A)$^{+}$ RNA from late stage pupae hybridized to probes prepared from the 1.5 kb *ctp* cDNA clone. Lane 1, Can-S RNA showing hybridization to 4.3 and 1.8 kb bands. Lane 2, RNA from *ctp*^{e73} showing no signal. The blot was intentionally overexposed to bring up any faint bands that might be in the *ctp*^{e73} lane. Uniformity of loading was determined by hybridization to a probe of the ribosomal protein gene rp49.

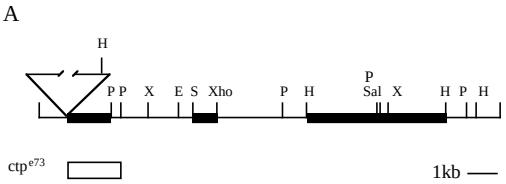

B

```
D. melanogaster   1    MSDRKAVIKNADMSEEMQQDAVDCATQALE 30
C. elegans             MVDRKAVIKNADMSDDMQQDAIDCATQALE
Chlamydomonas        MASGSSKAVIKNADMSEEMQADAVDCATQALE
                     ******          **  *  *

D. melanogaster  31   KYNIEKDIAAYIKKEFDKKYNPTWHCIVGR 60
C. elegans            KYNIEKDIAAYIKKEFDKKYNPTWHCIVGR
Chlamydomonas         KYNIEKDIAAYIKKEFDRKHNPTWHCIVGR
                                      * *

D. melanogaster  61   NFGSYVTHETRHFIYFYLGQVAILLFKSG 89
C. elegans            NFGSYVTHETKHFIYFYLGQVAILLFKSG
Chlamydomonas         NFGSYVTHETKHFIYFYLGQVAILLFKSG
                                    *
```

* nonconserved amino acids

Fig. 6. Restriction map of the genomic region containing the *ctp* gene. (A) The P element insertion site in *ctp*^{1} is shown as a broken triangle above the map. The regions that hybridize to the 1.5 kb cDNA clone are shown as a thick black line. The region deleted in the *ctp*^{e73} excision allele is shown as an open box below the map. Abbreviations: E, *Eco*RI; H, *Hin*dIII; P, *Pst*I; X, *Xba*I; S, *Sac*I. (B) Amino acid sequence comparison between *ctp* and the 8 kDa dynein light chain of *C. elegans* and Chlamydomonas. Nonconserved amino acids are denoted by an asterisk.

fail to complement the lethal and female-sterile phenotypes of *ctp* alleles. We also analyzed the sensory axon projections in strong alleles of *Ddlc1* and found they showed the same sensory axon projection defects that were observed for *ctp* mutants. Thus the 8 kDa dynein light chain gene in *Drosophila* is required for proper axon guidance of imaginal sensory neurons.

DISCUSSION

Mutations in *ctp* disrupt sensory axon projections but not target domains

We have characterized the role of a gene, called *cut up*, on axon trajectories in the imaginal nervous system. Mild alleles of *ctp* caused behavioral defects and female sterility, and null alleles were lethal and caused sensory axon defects. In severe alleles of *ctp*, the axons of leg sensory neurons followed abnormal pathways within the CNS. In the case of the tactile neurons, Murphey et al. (1989a) demonstrated that there are two main tracts and anterior and posterior paths. The *engrailed-lacZ* reporter ryXho25 (Hama et al., 1991) demonstrated that the axons of the posterior tactile neurons of the legs often chose the anterior trajectory that was inappropriate for neurons in the posterior compartment (Fig. 1). As Shepherd and his colleagues have demonstrated, there are a number of tracts that imaginal proprioceptive axons grow along, some of which are pioneered by persisting larval axons (Smith and Shepherd, 1996; Shepherd and Smith, 1996). Using two P[Gal4] enhancer trap insertions, we showed that the axons of the feCO club neurons often chose an abnormal anterior pathway (Fig. 2). The axons of the anterior chordotonal organ were often misrouted, running on a more anterior tract before projecting into their usual regions of the flight neuropil (Fig. 3). Finally, the axons of the claw femoral chordotonal neurons exhibited several defects, characterized by unusual branching and defasciculation (Fig. 3).

In spite of these axon trajectory errors, the sensory axons terminated in domains appropriate for neurons of their modality. The axons of the tactile neurons still terminated in the ventral region of the neuropil characteristic of tactile axons (Fig. 1B), albeit in a region characteristic of tactile neurons from more anterior locations on the leg. The axons of the feCO club neurons often followed an unusual ventral trajectory, but still terminated in the normal target area called mVAC (Fig. 2B). These results strongly suggest that the function of *ctp* in pathway choice is independent of the target recognition system. The sectioned material also suggests the relative normality of the target areas, which are still recognizable to the human observer as well as to the sensory neuron growth cones.

The locus of the defect and the nature of nervous system assembly

Our results suggest that the assembly of the imaginal sensory system can be described in a manner similar to that emerging for the larval neuromuscular junction. Analysis of the genes required for proper assembly of the synaptic connections at the larval neuromuscular junction reveal at least three distinct steps in the process: (1) pathfinding by motoneuron growth cones to the periphery; (2) selection of the group of muscles that are acceptable targets – the muscle domain and (3) recognition of specific target cells within a domain (van Vactor et al., 1993). Each of these steps requires the function of a different subset of genes. The genes *short stop* and *stranded* are required for the pathfinding step in the process and mutations in these genes cause growth cones to stall at choice points along the pathway before reaching their targets. Mutations in genes like *walkabout* and *clueless* are required for the final step in target recognition. In their absence growth cones make the proper pathfinding choices and reach the proper muscle domain, but then wander about apparently without choosing the appropriate target (Van Vactor et al., 1993). These mutations and a vast array of other data support the suggestion that the mechanisms of axon pathfinding are distinct from those involved in synaptic target recognition. As in the pathfinding mutants *shortstop* and *stranded*, the axon pathways in *ctp* are clearly disturbed. However, the synaptic domains within the CNS appear to be preserved in *ctp*. For each class of sensory axon we examined, the domain normally innervated appears to be intact, although the axon trajectory to arrive at that domain was often dramatically different in mutant specimens. We cannot yet tell whether the synaptic connections are normal. Such analyses will require the development of better assays for the underlying synaptic circuitry.

The defects we observe in the imaginal CNS imply that axon pathfinding has been disrupted by *ctp*. Although we see only the final result of the pathfinding process in our experiments, it will be possible to examine the process more directly by taking advantage of markers that label the axons during the pathfinding process. Shepherd and Smith (1996) have demonstrated the persistence of larval sensory neurons and their axons into the imaginal nervous system. These persisting neurons are likely to supply the scaffold of tracts available to in-growing axons of imaginal sensory neurons. We are using some of the lines to examine the development of the axon pathways in wild-type and mutant nervous systems to examine the behavior of growth cones at choice points.

Our results also raise the question of where the defect is localized. It is difficult at this stage in our work to determine whether the defect is in the sensory neurons themselves, in the central neurons, or in a combination of the two. The fact that the dynein light chain appears to be expressed in most cell bodies in the pupal CNS suggests that the defects could be a consequence of altered substrates in the CNS. It is possible that the pathways in the CNS are altered and sensory neurons simply make errors due to the altered substrate. In the present work we have focused on the sensory neurons. We are presently examining motor neurons in the imaginal nervous system to determine the extent of defects caused by the loss of the dynein light chain. There are a number of ways to determine the locus of the defect, either with mosaic analysis or by taking advantage of the P[Gal4] system to drive the *ctp* gene in sensory neurons in mutant backgrounds, and these experiments are underway.

Dynein light chain and axon pathfinding

Molecular analysis of the *ctp* mutation reveals that it encodes the 8 kDa dynein light chain gene (Fig. 6, see also Dick et al., 1996). This finding draws attention to the role that dynein and its molecular partners play in axon pathfinding. There are at least two classes of potential mechanism that could be important. First, dynein could function in the orientation of the cytoskeleton within the growth cone. For example, within the growth cone of grasshopper T1 neurons, microtubules selectively invade the

filopodia that will eventually become the new axon (Sabry et al., 1991). Upon selection of a particular direction of growth by the growth cone, the microtubule array changes from a scattered to a bundled arrangement, a transition that may require the function of the microtubule-associated motor proteins (Tanaka and Sabry, 1995; Tanaka and Kirschner, 1991; Sabry et al., 1991). Disruption of dynein function could affect this microtubule bundling and thereby affect directional axon growth.

In yeast, dynein loss of function mutations result in a failure of the spindle to orient properly during bud formation, a defect with the secondary effect of altering nuclear migration (Y.-Y. Li et al., 1993; M.-G. Li et al., 1994; Eshel et al., 1993). This orientation could involve the binding of dynein to microtubules associated with the spindle, and the movement of those microtubules to achieve proper spindle orientation. Similar binding and movement of microtubules could occur within growth cones to achieve microtubule orientation and affect the direction of migration.

If microtubule bundling is required for pathway choice, one could predict that the *ctp* mutation would shift growth cones to a 'random choice' mode, where mutant growth cones would be equally likely to take alternative pathways at particular choice points. Partial support for this model can be illustrated by the projections of the feCO club axons, which exhibited only two pathway choices (anterior or posterior). In the dynein light chain null mutants, these axons either projected normally (28/46 cases or 60.9%), were divided with some axons projected on both pathways (16/46 cases or 34.8%), or were all deflected to the anterior pathway (2/46 cases or 4.3%). The observed distribution is clearly not 'random' with respect to the choice of either the normal or the abnormal pathway. However, the distribution does fit the prediction made by a simple binomial distribution. In this model the axons of the feCO club neurons follow one of two independent pioneer neurons (Bate, 1976), and each pioneer has a chance of choosing the incorrect anterior pathway. If we set the chance of error at 22% for each pioneer, the model predicts 60.8% normal, 34.3% divided, 4.8% completely deflected, which fit the observed data very closely. Thus the loss of the dynein light chain increases the chance of errors, but fails to randomize completely the direction followed by these axons with respect to these two potential pathway.

However, the observed frequency of errors is not the same for each type of sensory neuron. The aCO projections follow unusual pathways in approximately 75% of the cases we scored (69/92). Further, the bundle of aCO axons was never observed to be divided between two pathways, suggesting that there is only one pioneer for this set of projections. The tactile projections identified by the ryXho25 marker also showed defects at a high frequency, greater than the 22% rate we observed for the club feCO axons. This means we cannot apply a single probability of error to all the mutant axons; however, the chance of error is increased with respect to wild type in all cases. The variable error rates suggest that different types of neurons may make use of the dynein light chain in different ways, and that some are more sensitive to its loss than others.

A second possible role for dynein is that mutants in the dynein light chain might disrupt retrograde axonal transport. Dynein functions as a minus-end-directed microtubule motor that transports vesicles toward the cell body (Schnapp and Reese, 1989; Vallee et al., 1989). Disruption of retrograde transport could alter either the movement of signaling molecules associated with the growth cone at certain stages of pathfinding, or the movement of structural molecules whose retrograde transport is important for axon directional changes.

Cytoplasmic dynein is likely to be required in all cells and strong loss of function alleles of the dynein heavy chain gene are larval lethals (McGrail et al., 1995; Gepner et al., 1996); clones of cells that have lost dynein heavy chain function also die (Gepner et al., 1996). However null mutations in the 8 kD dynein light chain are larval-viable and not lethal until late pupal development, suggesting that this subunit may not be required as a vital function in the same manner as the dynein heavy chain. Incomplete penetrance of the mutant phenotypes is observed in all of our assays, even though we are analyzing the effects of a null allele. This may be due to maternal effect of the product. The dynein heavy chain is packaged maternally into the egg and like the light chain, has a female-sterile phenotype (Gepner et al., 1996; McGrail et al., 1995). Maternal rescue of the dynein light chain mutations is a likely explanation for the difference between the penetrance of the axon projection in the embryonic CNS, where only about 11% of the preparations showed detectable defects, and the imaginal CNS, where a much higher percentage of the preparations of showed defects. The maternal contribution that may have rescued the embryonic axons could also explain the fact that, in the majority of our preparations, axons with abnormal trajectories are observed in CNS preparations that also contained axons with normal anatomy in adjacent neuromeres. This observation, however, also could be understood using the standard explanation that the components of axon pathfinding lost in *ctp* mutants involve functions for which some redundancy could exist. This redundancy is unlikely to involve other members of the dynein light chain gene family. In Drosophila, King and Patel-King (1995) have recently isolated two dynein light chain genes from Chlamydomonas with high homology, and two *Drosophila* light chain genes have been isolated as well. The *Drosophila* genes consist of the CNS-expressed 8 kD gene identified by the *ctp* mutation, and a second gene that is testis-specific and is associated with axonemal dynein which maps elsewhere in the genome (T. Hays, personal communication).

The dynein light chain is thought to interact with a variety of other cytoskeletal molecules in a protein complex crucial to cell shape and motility (Vallee and Sheetz, 1996). It may now be possible to dissect these interactions, particularly the role of the dynein light chain interactions, which is poorly understood, by creating double mutant animals with the dynein light chain and its putative molecular partners in the cytoskeleton.

We would especially like to thank Suman Reddy, Michael Getzinger William Irwin and Laura Smith who made the histological preparations used in this paper and Pamela Westgate and Sian Gramates who carried out much of the genetics. We would also like to thank David Shepherd who kindly involved us in screening the P[Gal4] lines and has provided continual contributions and discussion of the P[Gal4] work, Kim Kaiser for providing the P[Gal4] lines, Melody Siegler who provided the impetus to examine the imaginal CNS in the *en-lacZ* line where we first noticed the tactile afferent projections, and Carol Bigelow for discussions of the statistical model. We thank William Chia and Thomas Dick for communicating their unpublished results and for supplying the Ddlc mutants. Finally we thank, Patricia Wadsworth for valuable discussions about dynein, and Kai Zinn for the cDNA library. Supported by NIH grant NS15571 and NSF grant IBN 95-11338.

REFERENCES

Bate, C. M. (1976). Pioneer neurons in an insect embryo. *Nature* **260**, 54-56.

Bier, E., Vaessin, H., Shepherd, S., Lee, K., McCall, K., Barbel, S., Ackerman, L., Carretto, R., Uemura, T., Grell, E., Jan, L. Y. and Jan, Y. N. (1989). Searching for pattern and mutation in the Drosophila genome with a P-lacZ vector. *Genes Dev.* **3**, 1273-1287.

Brand, A. and Perrimon, N. (1993). Targeted gene expression as a means of altering cell fates and generating dominant phenotypes. *Development* **118**, 401-415.

Chiba A., Snow, P., Keshishian, H. and Hotta, Y. (1995). Fasciclin III as a synaptic target recognition molecule in Drosophila. *Nature* **374**,166-68.

Colamarino, S. A. and Tessier-Lavigne, M. (1995). The axonal chemoatractant netrin-1 is also a chemorepellent for trochlear motor axons. *Cell* **81**, 621-629.

Dick, T., K. Ray, H. K. Salz and Chia, W. (1996). Cytoplasmic dynein (ddlc-1). mutations cause morphogenetic defects and apoptiotic cell death in *Drosophila*. *Mol. Cell Biol.* **16**, 1966-1977.

Eshel, D., Urrestarazu, L. A., Vissers, S., Jauniaux, J-C., Van Vliet-Reedijk, J. C., Planta, R. J. and Gibbons, I. R. (1993). Cytoplasmic dynein is required for normal nuclear segregation in yeast. *Proc. Natl Acad. Sci. USA* **90**, 11172-11176.

Field, L. H. and Pfluger, H.-J. (1989). The femoral chordotonal organ: a bifunctional orthopteran (*Locusta Migratoria*) sense organ? *Comp. Biochem. Physiol.* **93A**, 729-743.

Fischbach, K. F. and Heisenberg, M. (1984). Neurogenetics and behavior in insects in mechanisms of integration in the nervous system. *J. Exp. Biol.* **112**, 65-94.

Gepner, J., Li, M., Ludmann, S., Kortas, C., Boylan, K., Iyaduria, S. McGrail, M. and Hays, T. S. (1996). Cyoplasmic dynein function is essential in Drosophila melanogaster. *Genetics* **142**, 865-878.

Grenningloh, G., Rehm, E. J. and Goodman, C. S. (1991). Genetic analysis of growth cone guidance in Drosophila: Fasciclin II functions as a neuronal recognition molecule. *Cell* **67**, 45-57.

Hama, C., Ali, Z. and Kornberg, T. B. (1991). Region-specific recombination and expression are directed by portions of the *Drosophila engrailed* promoter. *Genes Dev*. **4**, 1079-1093.

Hedgecock, E. M., Culotti, J. G. and Hall, D. H. (1990). The *unc-5*, *unc-6* and *unc-40* genes guide circumferential migrations of pioneer axons and mesodermal cells on the epidermis in *C. elegans*. *Neuron* **2**, 61-85.

Kania, A., Salzberg, A., Manzoor, B., D'Evelyn, D., Yuchun, H., Kiss, I. and Bellen H. J. (1995). *P*-Element mutations affecting embryonic peripheral nervous system development in *Drosophila melanogaster*. *Genetics* **139**, 1663-1678.

Kennedy, T. E., Serafini, T., dela Torre, J. R. and Tessier-Lavigne, M. (1994). Netrins are diffusible chemotropic factors for commissural axons in the embryonic spinal cord. *Cell* **78**, 425-435.

Killian, K. A., D. J. Merritt and R. K. Murphey (1993). Transplantation of neurons reveals processing areas and rules for synaptic connectivity in the cricket nervous system. *J. Neurobiol.* **24**, 1187-1206.

King, S. M. and Patel-King, R. S. (1995). The M_{rr} = 8,000 and 11,000 outer arm dyein light chains from *chlamydomonas* flagella have cytoplasmic homologues. *J. Biol. Chem*. **270**, 11445-11452.

Li, M.-G., McGrail, M., Serr, M. and Hays, T. S. (1994). *Drosophila* cytoplasmic dynein, a microtubule motor that is asymmetrically localized in the oocyte. *J. Cell Biol.* **126**, 1475-1494.

Li, Y.-Y., Yeh, E., Hays, T. and Bloom, K. (1993). Disruption of mitotic spindle orientation in a yeast dynein mutant. *Proc. Natl Acad. Sci. USA* **90**, 10096-10100.

Lin, D. M. and Goodman, C. S. (1994). Ectopic and increased expression of fasciclin II alters motoneuron growth cone guidance. *Neuron* **13**, 507-523.

Martin, K. A., Poeck, B., Roth, H., Ebens, A. J., Ballard, L. C. and Zipursky, S. L. (1995). Mutations disrupting neuonal connectivity in the Drosophila visual system. *Neuron* **14**, 229-240.

Matthes, D. J., Sink, H., Kolodkin, A. L. and Goodman, C. S. (1995). Semaphorin II can function as a selective inhibitor of specific synaptic arborizations. *Cell* **81**, 631-639.

McIntire, S. L., Garriga, G., White, J., Jacobson, D. and Horvitz, R. (1992). Genes necessary for directed axonal elongation or fasciculation in C. elegens. *Neuron* **8,** 307-322.

McGrail, M., Gepner, J., Silvanovich, A. Ludman, S., Serr, M. and Hays, T. S. (1995). Regulation of cytoplasmic dynein function in vivo by the Drosophila Glued complex. *J. Cell Biol.* **131**, 2: 411-425.

Merritt, D. and Murphey, R. K. (1992). Projections of leg proprioceptors within the CNS of the fly Phormia in relation to the generlaized insect ganglion. *J. Comp. Neurol.* **322**, 16-34.

Murphey, R. K., Possidente, D. R., Vandervorst, P. and Ghysen, A. (1989a). Compartments and the topography of leg afferent projections in Drosophila. *J. Neurosci.* **93**, 209-3217.

Murphey, R. K., Possidente, D. R., Pollack, G. and Merritt, D. J. (1989b). Modality-specific axonal projections in the CNS of the flies phormia and Drosophila. *J. Comp. Neurol.* **290**,185-200.

Nose, A., Mahajan, V. B. and Goodman, C. S. (1992). Connectin: a homophilic cell adhesion molecule expressed on a subset of muscles and the motoneurons that innervate them in Drosophila. *Cell* **70**, 553-567.

Pfluger, H. J., Braunig, P. and Hustert, R. (1988). The organization of mechanosensory neuropiles in locust thoracic ganglia. *Phil. Trans. T. Soc. Lond. B* **321**, 1-26.

Phillis, R. W., Bramlage, A. T., Wotus, C., Whittaker, A., Gramates, L. S., Seppala, D., Farahanchi, F., Caruccio, P. and Murphey, R. K. (1993). Isolation of mutations effecting neural circuitry required for grooming behavior in *Drosophila melanogaster*. *Genetics* **133**, 581-592.

Power, M. E. (1948). The thoracico-abdominal nervous system of an adult insect, *Drosophila melanogaster*. *J. Comp. Neurol.* **88**, 347-409.

Robertson, H. M., Preston, C. R., Phillis, R. W., Johnson-Schlitz, D. M., Benz, W. K. and Engels, W. R. (1988). A stable genomic source of P element transposase in *Drosophila melanogaster*. *Genetics* **118**, 461-470.

Sabry, J. H., O'Connor, T. P., Enans, L., Torian-Raymond, A.,Kirschner, M. W. and Bentley, D. (1991). Microtubule behavior during the guidance of pioneer neuron growth cones in situ. *J. Cell Biol.* **115**, 1381-1395.

Salzberg, A., D'Evelyn, D., Schulze, K. L., Lee, J.-K., Strumpf, D., Tsai, L. and Bellen, H. J. (1994). Mutations effecting the pattern of the PNS in Drosophila reveal novel aspects of neuronal development. *Neuron* **13,** 269-287.

Sambrook, J., Fritsch, E. F. and Maniatis, T. (1989). *Molecular Cloning; A Laboratory Manual*, 2nd edition. Cold Spring Harbor Laboratory Press.

Schnapp, B. J. and Reese, T. S. (1989). Dynein is the motor for retrograde axonal transport of organelles. *Proc. Natl Acad. Sci. USA* **86,** 1548-1552.

Seeger, M. A., Tear, G., Ferres-Marco, D. and Goodman, C. S. (1993). Mutations affecting growth cone guidance in Drosophila: genes necessary for guidance toward or away from the midline. *Neuron* **10**, 409-426.

Shepherd, D. and Smith, S. A. (1996). Central projections of persistent larval sensory neurons prefigure adult sensory pathways in the CNS of Drosophila. *Development* (in press).

Smith, S. A. and Shepherd, D. (1996). The central afferent projections of proprioceptive sensory neurons in *Drosophila* revealed with the enhancer trap technique. *J. Comp. Neurol.* **369**, 311-323.

Siegler, M. V. S., Pankhaniya, R. P. and Campbell, H. R. (1993). Expression of engrailed in identified neurons of the grasshopper CNS. *Soc. Neurosci. Abstr.*

Tanaka, E. and Kirschner, M. (1991). The role of microtubules in grwoth cone turning at substrate boundaries. *J. Cell Biol.* **128**, 127-137.

Tanaka, E. and Sabry, J. (1995). Making the connection: cytoskeletal rearrangements during growth cone guidance. *Cell* **83**, 171-176.

Thomas, J. B. and Wyman, R. J. (1982). Normal and mutant connectivity between identified neurons in Drosophila. *Trends Neurosci.* **6**, 214-219.

Trimarchi, J. R. and Murphey, R. K. (1995). Intracellular recording from and dye injection of neurons in the thoracic ganglia of adult Drosophila. *Soc. Neurosci. Abstr.* **21**, #175. 8.

Van Vactor, D., Sink, H., Fambrough, D., Tsoo, R. and Goodman, C. S. (1993). Genes that control neuromuscular specificity in Drosophila. *Cell* **73**, 1137-1153.

Vallee, R. B., Shpetner, H. S. and Paschal, B. M. (1989). The role of dynein on retrograde axonal transport. *Trends Neurosci.* **12**, 66-70.

Vallee, R. and Scheetz (1996). Targeting of motor proteins. *Science* **271**, 1539-1544.

(Accepted 10 July 1996)